ELSEVIER

Thermochimica Acta 276 (1996) 91–103

thermochimica acta

Thermal analysis of cation-exchanged zeolites before and after their amorphization by ball milling

Cleo Kosanović *, Boris Subotić, Ankica Čižmek

Ruđer Bošković Institute, P.O. Box 1016, 10000 Zagreb, Croatia

Received 8 May 1995; accepted 14 November 1995

Abstract

Zeolite X, synthetic mordenite and zeolite A in which a part of the original sodium ions has been exchanged by other cations (Li^+, K^+, Cs^+) were investigated by means of simultaneous thermal analysis, before and after mechanochemical amorphization by ball milling. In all the examined cases, the initial rate of dehydration of amorphized sample was higher than the initial rate of dehydration of the original (crystalline) samples, and the temperature at which the rate of dehydration is largest was lower in the case of the amorphized samples than in the case of the crystalline samples.

The influence of cations on the rate of dehydration and on the critical temperature of dehydration of amorphized samples was different from the influence of cations on the rate of dehydration and on the critical temperature of dehydration of the original (crystalline) samples. Analysis of the experimental data led to the conclusion that the rate of dehydration of crystalline samples is controlled by the diffusion of desorbed water through the channel/void system of the zeolite structure and that the rate of dehydration of the amorphized samples is controlled by the cation–water interactions. The observed differences are explained by the difference in the pore system between the original (crystalline) and amorphized samples.

Keywords: Amorphization; Ball milling; Cation exchange; Thermal analysis; Zeolites

1. Introduction

Thermal analysis has frequently been used for the characterization of different kinds of minerals, including zeolites and clays [1–3]. The results of simultaneous thermal

* Corresponding author. Tel.: 385 14561184; Fax: 385 1425497.

Elsevier Science B.V.
SSDI 0040-6031(95)02792-0

analysis can give very useful quantitative and/or semi-quantitative information on the processes of dehydration and thermal stability of different types of zeolites [4–7].

In addition, thermal analysis is a very sensitive method for the detection of very small structurally ordered units having a zeolite structure, distributed through the matrix of aluminosilicate gels [8,9].

Studying the cited papers, it can be concluded that the results of thermal analysis are very sensitive to the nature of the cations present in the aluminosilicate environment and to the interactions of the cations with the zeolite framework. Consequently, the results of thermal analysis can give useful information on the pore structure, catalytic activity, degree of hydration of the cations in the structure of the zeolites and amorphous aluminosilicates, interactions of hydrated cations with aluminosilicate matrix, etc.

Taking into consideration the drastic structural changes of the zeolite framework during its mechanochemical treatment [10–12] and the influence of cations on the observed changes [12,13], one can assume that the mechanochemical amorphization of zeolites considerably changes the interactions between the cations and the aluminosilicate matrix of the treated zeolites. In order to determine the nature of the assumed changes, original and mechanochemically treated zeolites (NaA, (Li,Na)A, (Na,K)A, (Na,Cs)A, NaX and Na-synthetic mordenite) were simultaneously analysed by the methods of thermogravimetry (TG), differential thermogravimetry (DTG) and differential scanning calorimetry (DSC).

2. Experimental

All the zeolites (Linde 4A, Linde 13X, synthetic mordenite) used as starting materials were products of Union Carbide Corp. Analytical grade LiCl, KCl, and CsCl were used for preparing 0.5 M solutions of lithium chloride, potassium chloride and caesium chloride, respectively.

Partial exchange of original Na^+ ions from zeolite A with Li^+, K^+ and Cs^+ ions from 0.5 M LiCl, KCl and CsCl solutions was carried out by the method described earlier [13]. The exchanged zeolites were kept in a desiccator with saturated NaCl solution for 24 h before analysis.

The chemical composition of the exchanged zeolites was determined by dissolution of the solids in concentrated HNO_3 and/or by the digestion with concentrated HF. The concentrations of silicon, aluminium and alkali ions in the solutions obtained by the dissolution of the solids, were measured using a Shimadzu AA-660 atomic absorption/flame emission spectrophotometer [13].

The samples of hydrous zeolites 4A, 13X and synthetic mordenite, as well as the samples obtained by partial exchange of Na^+ ions from zeolite 4A with Li^+, K^+, and Cs^+ ions from solution, were milled in a planetary ball mill (Fritsch Pulverisette type 7) at room temperature. For this purpose, a certain amount of each sample was put in an agate vessel containing 10 wolfram carbide balls ($\phi = 10$ mm), and then the vessel was rotated (speed of rotation, 3000 rpm) until the crystalline storing powder was completely transformed into X-ray amorphous material (2 h for zeolites A and X and 3 h for synthetic mordenite) [10,11,13]. The process of amorphization was followed by powder

X-ray diffractometry (Philips PW 1820 vertical goniometer with CuKα graphite radiation) [10,11,13]. Depending on the duration of milling, the outer temperature of the vessel can be increased to 40–60°C. The samples amorphized by ball milling were kept in a desiccator with saturated NaCl solution for 24 h before analysis.

Thermal analyses of the samples were performed on a Netzch STA 409 simultaneous thermal analysis apparatus. The heating rate was 10 K min^{-1} in nitrogen atmosphere. The flow rate of nitrogen was 15 cm^3 min^{-1}. The samples were heated in a platinum crucible ($\phi = 6.8$ mm, $L = 2.6$ mm). About 30 mg of sample was used in each run. Calcined kaolinite was used as a reference.

3. Results

Fig. 1 shows the relative loss of weight of the original (crystalline, solid curves) and milled (fully amorphized, dashed curves) samples of zeolite 4A (Fig. 1A), zeolite 13X (Fig. 1B) and synthetic mordenite (Fig. 1C) during their controlled heating in nitrogen atmosphere (heating rate, 10 K min^{-1}; flow rate of nitrogen, 15 cm^3 min^{-1}). The loss of weight was caused by the thermally induced desorption of moisture and zeolitic water (hydration shell of the Na^+ ions positioned on specific sites in the zeolite structure). In all cases, the rate of dehydration initially increased with increasing temperature of heating, reached a maximum at $T > 100$°C, and thereafter the rate of dehydration gradually decreased with increasing temperature, T. The initial weight loss of the samples, below 100°C, can be attributed to the desorption of physically absorbed water (moisture) from within the solid microstructure [9]. Depending on the type of zeolite, the dehydration was completed at about $T = 800$–1000°C. The water content in the fully amorphized samples is lower than in the original powders of zeolites 4A and 13X (see Table 1). This is in accordance with the discovery that the water content is lower in the amorphous aluminosilicates (gels) than in the crystalline ones (zeolites) [9]. Fig. 1A shows that the initial rate of dehydration of the amorphized zeolite A (dashed curve) is higher than the rate of dehydration of the original (crystalline) sample (solid curve). However, for $T > 200$°C, the rate of dehydration of the amorphized sample became lower than the rate of dehydration of the crystalline sample. In the case of zeolite X (Fig. 1B), the rate of dehydration of the amorphized sample (dashed curve) is approximately the same as the rate of dehydration of the original (crystalline, solid curve) sample up to $T \simeq 200$°C; thereafter the rate of dehydration of the amorphized sample was lower than that of the crystalline sample. The difference in the rate of dehydration between the original (crystalline) and the amorphized sample of the synthetic mordenite was not significant (see Fig. 1C).

The temperature T_m of the endothermic minimum in the DSC curves coincides with the temperature at which the rate of dehydration is maximal (see Figs. 1 and 3).

Here it is interesting that the endothermic minima in the DSC curves of the amorphized samples appears at lower temperatures, T_m, than the corresponding endothermic minima in the DSC curves of the original crystalline samples (see Figs. 2 and 3). For instance, the temperatures of the endothermic minima in the DSC curves of the original crystalline samples of zeolites 4A and 13X were 179 and 140°C,

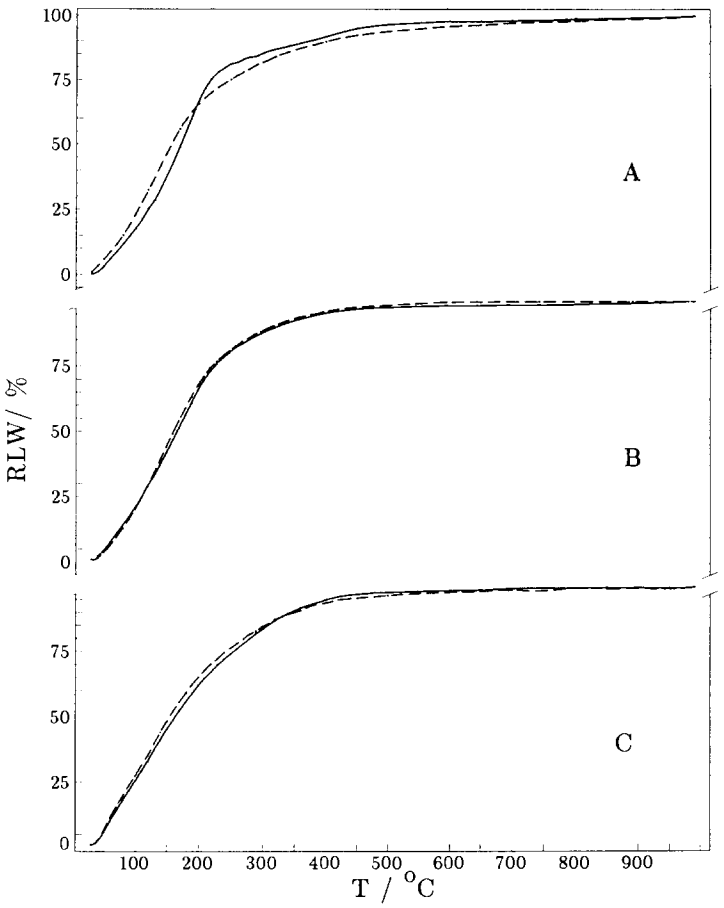

Fig. 1. Relative loss of weight, RLW, during the controlled heating of: A, original crystalline (solid curve) and amorphized (dashed curve) zeolite 4A; B, original crystalline (solid curve) and amorphized (dashed curve) zeolite 13X; and C, original crystalline (solid curve) and amorphized (dashed curve) synthetic mordenite. RLW = 100LW/TLW, where LW is the loss of weight at temperature T and TLW is total content of water in the sample (see Table 1).

respectively, while the temperatures of the endothermic minima in the DSC curves of the amorphous phases obtained by ball milling zeolites 4A and 13X were 127 and 111°C, respectively. Exothermic peaks in the DSC curves of zeolites 4A (Fig. 2A) and 13X (Fig. 3A) above 800°C, correspond to high-temperature solid-state transformations. Amorphization of the synthetic mordenite had no significant effect on its behaviour during the controlled heating, i.e. the DSC and DTG curves of the amorphized sample were almost identical to the DSC and DTG curves of the crystalline sample.

The maximum theoretical cation-exchange capacity of zeolite A is approx. $5.5 \times 10^{-3}/n$ mol g^{-1}, where n is the charge of the exchange cations from the liquid

Table 1
Total content of water (wt%) in crystalline and amorphized samples of zeolites 4A, 13X and synthetic mordenite

Type of zeolite	Crystalline	Amorphized
4A	20.17	16.86
13X	23.01	15.44
Synthetic mordenite	14.12	14.62

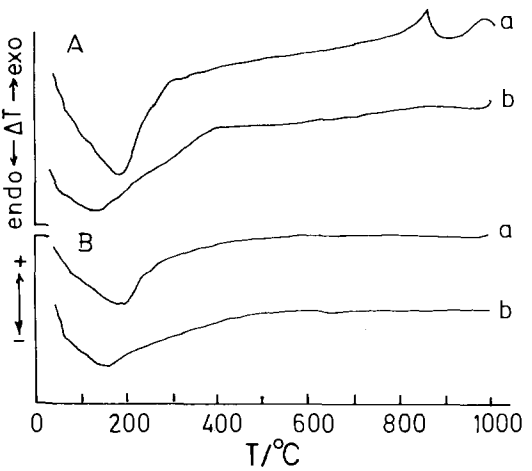

Fig. 2. DSC (A) and DTG (B) curves of original crystalline (a) and amorphized (b) samples of zeolite 4A.

phase. However, in most real cases, only a part of the Na^+ ions from the zeolite can be exchanged with the ions from solution. The fraction f_{R+} of the exchanged cations depends on the chemical nature of the exchangeable cations and on the physical and chemical conditions under which the exchange process is carried out [14,15]. Table 2 shows the fractions f_{Na+} of the Na^+ ions and, f_{R+} of the R^+ ions (R^+ being Li^+, K^+, Cs^+) contained in the zeolite A after partial exchange of original Na^+ ions from zeolite A with R^+ ions from solution, by the procedure described in the Experimental Section, above.

Partial exchange of the sodium ions in zeolite 4A with other cations (Li^+, K^+, Cs^+) did not affect the basic structure of the zeolite A framework or the cell constant, except in the case of the lithium-exchange zeolite A, as revealed by X-ray powder diffractometry and FTIR spectroscopy [13].

The lowering of the cell constant in the case of zeolite A in which a part of the Na^+ ions has been exchanged by Li^+ ions, was explained by the distortion of the zeolite framework caused by strong electrostatic interaction between the zeolite framework and the small, strongly polarizing Li^+ ion [13,16–19].

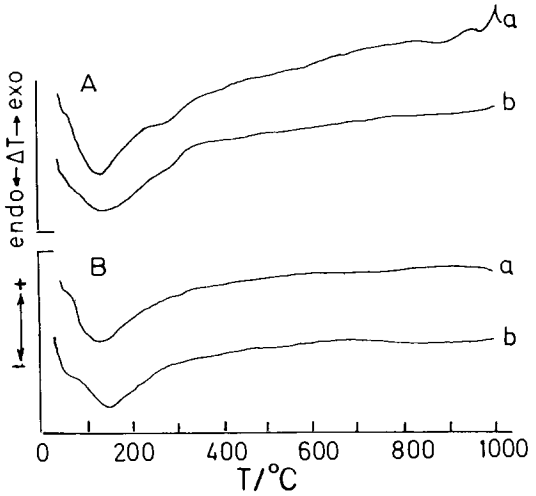

Fig. 3. DSC (A) and DTG (B) curves of original crystalline (a) and amorphized (b) samples of zeolite 13X.

Table 2
Fractions, f_{Na}, of Na^+ ions and f_{R^+}, of R^+ ions and the ratio between Na^+ and R^+ ions in the exchanged zeolite A

Cation R^+	f^+_{Na}	f^+_R	f^-_{Na}/f^-_{Na}
Li^+	0.36	0.64	0.56
Na^+	1.00	0.00	1.00
K^+	0.22	0.78	0.28
Cs^+	0.66	0.34	1.94

Kinetic analysis of the amorphization of exchanged zeolite A showed that the change of fraction, f_a, of the amorphous phase obtained during the ball milling of the exchanged zeolites can be expressed by the equation [13]

$$f_a = 1 - \exp(-kt_m) \quad (1)$$

where t_m is the time of milling and k is the rate constant. This means that a partial exchange of sodium with Li^+, K^+, and Cs^+ ions did not affect the basic mechanism of the amorphization process, but only the rate of amorphization as indicated by the influence of the type of exchanged cations on the constant rate k. The values of k lie between 1.63 h^{-1} (for potassium exchanged zeolite A) and 3.45 h^{-1} (for the original sodium form of zeolite A) (see Table 3 in Ref. [13]).

Figs. 4 and 5 show the DSC and DTG curves of the original powder (sodium form) of zeolite 4A (curves b in Figs. 4A and 5A) and of lithium-exchanged (a), potassium-exchanged (c) and caesium-exchanged (d) zeolite A , before (A) and after (B) amorphization by ball milling.

Table 3
Temperatures, T_m (°C), of the minima in DSC and DTG curves of crystalline and amorphized samples of zeolite A in which a part of the original sodium ions has been exchanged by Li^+, K^+ and Cs^+ ions

Cations	Crystalline samples		Amorphized samples	
	DSC	DTG	DSC	DTG
Na^+, Li^+	138.6	140	54.0, 84.9	100
Na^+	140.6	145	110.9	130
Na^+, K^+	142.1	160	82.8	98
Na^+, Cs^+	128.1	130	81.2	95

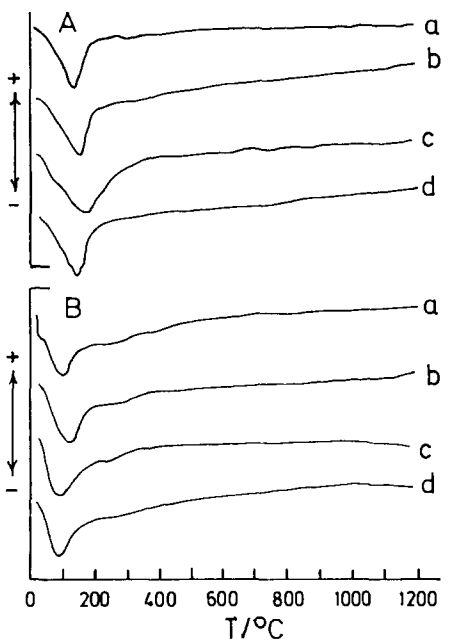

Fig. 4. DSC curves of: A, original crystalline; and B, amorphized samples of zeolite A in which a part of the original sodium ions has been exchanged by Li^+ (a), K^+ (c) and Cs^+ (d) ions. DSC curves (b) correspond to original crystalline (A) and amorphized (B) samples of zeolite 4A (sodium form).

The DSC curves of both crystalline (Fig. 4A) and amorphized (Fig. 4B) samples are characterized by an endothermic minimum at $100°C < T < 200°C$ for crystalline samples, and below 100°C for amorphized samples, and by one or two exothermic peaks at temperatures above 800°C (DSC curves of both crystalline and amorphized lithium-exchanged zeolite A also have an endothermic minimum at $T \simeq 1150°C$, see curve a in Fig. 4). The minima in the DSC and DTG curves for the amorphized samples appear at lower temperatures, T_m, than the corresponding minima in the DSC and DTG curves of the original crystalline samples (see Table 3 and Figs. 4 and 5).

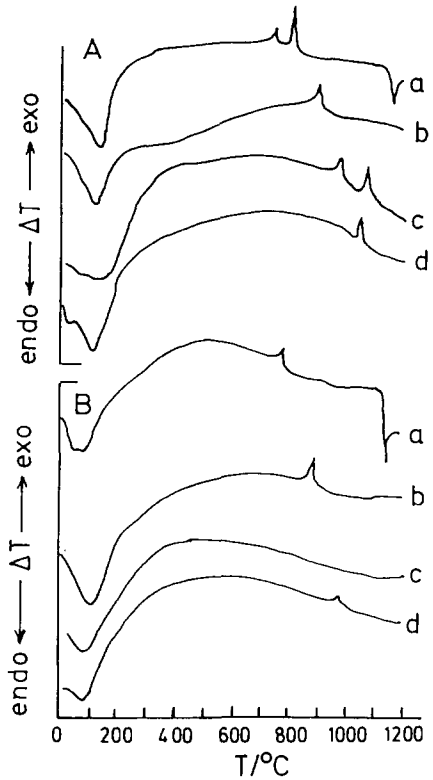

Fig. 5. DTG curves of: A, original crystalline; and B, amorphized samples of zeolite A in which a part of the original sodium ions has been exchanged by Li^+ (a), K^+ (c) and Cs^+ (d) ions. DTG curves (b) correspond to original crystalline (A) and amorphized (B) samples of zeolite 4A (sodium form).

As expected, the temperatures T_m of the low- temperature endothermic minima coincide with the temperatures of the minima in the corresponding DTG curves (see Table 3 and Figs. 4 and 5).

As already indicated, the initial water content in the fully amorphized samples is lower than in the corresponding crystalline samples (see Table 4).

4. Discussion

It is well known that the appearance of an endothermic minimum during controlled heating of zeolites is a consequence of the consumption of the thermal energy needed for dehydration of the hydrated cations positioned in the zeolite framework and the release of water molecules from the channel/void system of the zeolite structure [14,16–18].

Table 4
Total amount of water (wt%) in crystalline and amorphized samples of zeolite A in which a part of the original sodium ions has been exchanged by Li^+, K^+ and Cs^+ ions

Cations	Crystalline	Amorphized
Na^+, Li^+	20.86	16.86
Na^+	20.17	16.83
Na^+, K^+	16.83	13.61
Na^+, Cs^+	13.83	13.42

Based on the considerations that: (1) the electrostatic potential [20] and the energy of hydration [21] of the cation increase with decreasing ionic radius, and (2) the energy needed to release water molecules from the channels decreases with increasing effective diameter of the channels, one can assume that the rate of dehydration would increase and the temperature, T_m, would decrease with both the increase of the effective diameter, D, of the channels and with the increase of the ionic radii of the hydrated cations present in the zeolite structure. Hence, the lower value of T_m in the DSC curve of zeolite 13X ($T_m = 140°C$;, see curve a in Fig. 3A) than in the DSC curve of zeolite 4A ($T_m = 179°C$;, see curve a in Fig. 2A) can be readily explained by the fact that the effective diameter of the channels of zeolite 13X is larger ($D = 0.74$ μm) than that of zeolite A ($D = 0.41$ μm).

The lack of any influence of the amorphization of synthetic mordenite on the rate of dehydration is probably related to the specific structure of the mordenite framework (a system of parallel, unconnected channels) but at present this is an unproved thesis that should be confirmed or rejected in a separate study.

However, the deviation in the rate of dehydration of the exchanged zeolite A (see Fig. 6) from the simple rule based on electrostatic interactions only, leads to an assumption that the rate of dehydration of the crystalline samples is influenced not only by the water–ion electrostatic interaction, but also that the interactions between the hydrated cation and aluminosilicate framework have to be considered.

It is well known that hydrated cations occupy specific sites in the channels and voids of the zeolite framework. These sites correspond to the minimum energy of interaction between the hydrated cation and the aluminosilicate framework of the zeolite structure [22].

In the unit cell of zeolite 4A (NaA), eight of the twelve sodium ions are located near the centre of 6-rings on the 3-fold axis inside the α-cage, called the S_I sites. The remaining four ions are less localized in the dehydrated zeolite. They are thought to be situated adjacent to the eight-membered windows, called site S_{II}, controlling the access of the α-cages. Hence, partial exchange of the sodium ions situated on site S_{II} by smaller lithium ions results in a widening of the effective pore size, while the partial exchange of the sodium ions by larger potassium or caesium ions causes a narrowing of the effective pore size.

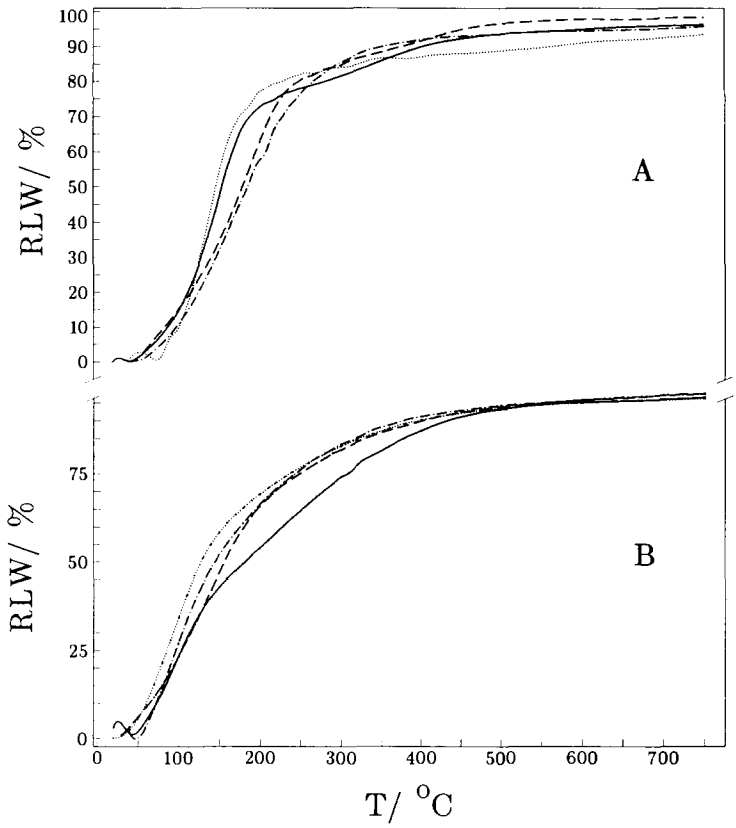

Fig. 6. Relative loss of weight, RLW, during the controlled heating of original crystalline (A) and amorphized (B) samples of zeolite A in which a part of the original sodium ions has been exchanged by Li^+ (–), K^+ (– –), and Cs^+ (. . .) ions. Dashed curves (---) correspond to the RLW of the original (A) and amorphized (B) samples of zeolite 4A (sodium form).

Taking into consideration these effects, the results presented in Figs. 4–6 can be explained as follows. The largest rate of dehydration, and consequently, the lowest temperature of dehydration of caesium-exchanged zeolite A are consequences of the weak electrostatic interaction between the structure-breaking caesium ion and the water molecules. Although the caesium ion is the largest of those examined, the relatively low degree of its hydration as well the relatively low degree of its exchange ($f_{Cs+} = 0.34$, see Table 2) means that the narrowing of the effective channel diameter is not significant relative to the effective channel diameter of the pure sodium form of zeolite A.

However, despite strong electrostatic interaction between lithium ions and water molecules [19], the relatively high rate of dehydration of the sample in which a part of the sodium ions was exchanged with smaller lithium ions, leads to an assumption that a larger amount of energy is spent on the diffusion of water molecules through the

channel/void system of the zeolite structure than on the dehydration of the hydrated ions.

A similar conclusion was drawn from the results of simultaneous thermal analysis of amorphous aluminosilicate gels that contain various mixtures of sodium, potassium and lithium ions [9].

In this context, the decrease of the rate of dehydration in the sequence $J_{Na,Cs} > J_{Na,Li} > J_{Na} > J_{Na,K}$ (see Fig. 6A) is logical and expected, taking into consideration the different size, degree of hydration and degree of exchange, as well as the previously explained deviation in the case of caesium-exchanged zeolite A.

The rate of dehydration of the amorphized samples (see Fig. 6B) depends on the type of cation present in the aluminosilicate matrix in a different way than the rate of dehydration of the original (crystalline) samples (see Fig. 6A).

The temperatures, T_m, of the endothermic minima in the DSC and DTG curves of the amorphized samples are below 100°C (see Figs. 4B and 5B, and Table 3) indicating that the initial rate of dehydration of the amorphized samples is higher than the initial rate of dehydration of the crystalline ones (see Fig. 6). This indicates that the thermal properties of the amorphized samples are more similar to the thermal properties of precipitated amorphous aluminosilicate gels [9] than to those of the original crystalline phases. An earlier mechanochemical study of zeolite A showed that the exterior surface area of zeolite A was duplicated during the amorphization by ball milling [12]. Hence, the higher rate of water desorption from the amorphized samples than from the crystalline ones may be ascribed to the increase in the exterior surface area during the amorphization. However, knowing that the hydrated cations are distributed through the entire mass (volume) of both crystalline and amorphized samples and that the exterior surface area of zeolites is considerably lower than the internal surface area, one can assume that the decrease in T_m (see Table 3) and the increase in the rate of water desorption (see Fig. 6) are caused not only by the increase in the exterior surface area but also by the destruction of the original crystal structure of zeolite and the increasing of the pore size during amorphization [10–14]. An increase in the rate of dehydration in the sequence: $J_{Li,Na} < J_{Na} < J_{Na,K} < J_{Na,Cs}$, i.e. with the increase in the ionic radius of the exchanged ion ($r_{Li+} < r_{Na+} < r_{K+} < r_{Cs+}$) corroborates such an assumption.

Therefore, the energy of dehydration of the cation decreases with the increase in the ionic radius of the cation and, hence, it can be concluded that in the case of amorphized samples the rate of dehydration is controlled by the electrostatic interaction (the strength of the bond) between ion and water molecules through the pore system of the examined materials.

Assuming that the effective size of the pores formed by destroying the original zeolite structure is considerably larger than the size of the hydrated cations, the size of the cation does not markedly affect the diffusion of desorbed water molecules through the pore system, and hence the dominant factor that controls the rate of dehydration is just the strength of the electrostatic force between cation and water molecules.

Although this thesis explains the observed effects in a satisfactory way, it will be fully confirmed, reconsidered, or even rejected in our further studies on the fine structure of the amorphized zeolites.

5. Conclusion

Results of simultaneous thermal analysis of zeolites 4A, 13X and synthetic mordenite, before and after amorphization by ball milling, showed that: (1) the initial rate of dehydration of the original (crystalline) zeolite 4A (sodium form) is slower than the initial rate of dehydration of the amorphized sample, and after $T > 200°C$, the rate of dehydration of the crystalline sample is higher than that of the amorphous sample; (2) the initial rate of dehydration of the original zeolite 13X is almost the same as that of the amorphous sample, and after $T > 200°C$, the rate of dehydration of the crystalline sample is higher than that the amorphous sample; (3) there is no significant difference in the rate of dehydration between the original (crystalline) and amorphized sample of synthetic mordenite; and (4) endothermic minima in the DSC and DTG curves of the amorphized samples appear at lower temperatures than the corresponding endothermic minima in the DSC and DTG curves of the original crystalline samples. The observed effects can be explained by the thesis that the energy needed for the removal of water molecules from the pores formed during the amorphization is lower than the energy needed for the removal of water molecules from the channel/void system of the original crystalline zeolites.

The rate of dehydration of the samples of zeolite A in which a part of the original sodium ions have been exchanged by Li^+, K^+ and Cs^+ ions decreased in the sequence: $J_{Na,Cs} > J_{Na,Li} > J_{Na} > J_{Na,K}$, while the rate of dehydration of the corresponding amorphized samples decreased in the sequence: $J_{Na,Cs} > J_{Na,K} > J_{Na} > J_{Na,Li}$. This indicates that the rate of dehydration of the original (crystalline) zeolite A is controlled by the diffusion of desorbed water molecules through the channel/void system of the zeolite structure, and thus also by the size of the hydrated cations, while the rate of dehydration of amorphized samples is controlled by electrostatic interaction (the strength of the bond) between ion and water molecules, rather than by the diffusion of the desorbed water molecules through the pore system of the examined materials.

Acknowledgments

The authors thank the Ministry of Science and Technology of the Republic of Croatia for its financial support.

References

[1] R.C. Mackenzie, in R.C. Mackenzie (Ed.), Differential Thermal Analysis, Vol. 1, Academic Press, London, (1970) 498.
[2] W. Smykatz-Kloss, Differential Thermal Analysis, Application and Results in Mineralogy, Springer-Verlag, Berlin, (1974) 81.
[3] D.N. Todor, Thermal Analysis of Minerals, Abacus Press, Tunbridge Wells, Kent, UK, (1976) 208.
[4] H.G. McAdie, in R.C. Mackenzie (Ed.), Differential Thermal Analysis, Vol. 1, Academic Press, London, (1970) 449.
[5] C.V. McDaniel and P.K. Maher, in J.A. Rabo (Ed.), Zeolite Chemistry and Catalysis, ACS Monograph 171, American Chemical Society, Washington, DC, (1976) 258.

[6] E.N. Shylyapkina, J. Therm. Anal., 13 (1978) 553.
[7] H.W. Haynes, Catal. Rev. Sci. Eng., 17 (1978) 283.
[8] Z. Gabelica, J.B. Nagy, E.G. Deroane and J.-P. Gilson, Clay Minerals, 19 (1984) 803.
[9] R. Aiello, F. Crea, A. Nastro, B. Subotić and F. Testa, Zeolites, 11 (1991) 767.
[10] C. Kosanović, J. Bronić, B. Subotić, I. Šmit, M. Stubičar, A. Tonejc, and T. Yamamoto, Zeolites, 13 (1993) 261.
[11] C. Kosanović, J. Bronić, A. Čizmek, B. Subotić, I. Šmit, M. Stubičar and A. Tonejc, Zeolites, 15 (1995) 45.
[12] C. Kosanović, A. Čizmek, B. Subotić, I. Šmit, M. Stubičar and A. Tonejc, Zeolites, 15 (1995) 51.
[13] C. Kosanović, A. Čizmek, B. Subotić, I. Šmit, M. Stubičar and A. Tonejc, Zeolites, accepted.
[14] D.W. Breck, Zeolite Molecular Sieves, Wiley and Sons, New York.
[15] D.W. Breck, W.G. Eversole, R.M. Milton, T.B. Reed and T.L. Thomas, J. Am. Chem. Soc., 78 (1956) 5963.
[16] P.C. Borthakur and B.D. Chattaray, J. Therm. Anal., 17 (1979) 67.
[17] A.J. Chandwadakar and S.B. Kulkarni, J. Therm. Anal., 19 (1980) 313.
[18] B.L. Yu, A. Dyer and H. Enamy, Thermochim. Acta, 200 (1992) 299.
[19] P.K. Dutta and B. Del Barco, J. Phys. Chem., 108 (1986) 1861.
[20] V. Ramamurthy, D.R. Sanderson and D.F. Eaton, Photochem. Photobiol., 56 (1992) 297.
[21] L.I. Antropov, Theoretical Electrochemistry, Mir Publishers, Moscow, (1972), p. 69.
[22] R.M. Barrer, L.V.C. Rees and M. Shamsuzzoha, J. Inorg. Nucl. Chem., 28 (1966) 629.